Available online at www.sciencedirect.com
SCIENCE DIRECT®
Physica E 19 (2003) 251–256
PHYSICA E
www.elsevier.com/locate/physe

Thermal degradation of semiconductor qubit inverter operation in narrow band-gap materials

M.J. Gilbert*, R. Akis, D.K. Ferry

Department of Electrical Engineering and Center for Solid State Electronics Research, Arizona State University, Tempe, AZ 85287-5706, USA

Abstract

Recently, quantum computing has received a great deal of focus as a possible means of achieving rapid computational speeds when compared with that of classical computation. Nonetheless, in many of the current implementations of a "quantum computer", the semiconductor platform has been largely overlooked. It has been previously demonstrated that it is possible to form the NOT gate in a coupled semiconductor waveguide structure in III–V materials. However, to this point, investigations have not included the effects of non-zero temperature on the system. It is crucial to determine what effect temperature has on the system. We present results of a semiconductor waveguide inverter in GaAs and InAs with non-zero thermal effects included in the simulation. The behavior of the device clearly shows that with the inclusion of thermal effects in these materials, waveguide NOT gate function is still possible. Nevertheless, care must be taken when selecting the operational values of the inverter as shifts in the I–V curves occur which could cause unwanted operation of the inverter.
© 2003 Elsevier B.V. All rights reserved.

Keywords: Quantum computing; Qubit; Thermal effects; Waveguide inverter

Much of quantum computation and information theory has been structured around the use of the qubit. Two or more bits of quantum information are coupled together to achieve basic logic structures for subsequent processing, whereby the most basic and essential coupling of qubits is the controlled not gate (CNOT). Before a CNOT construct can be realized, we must first demonstrate the operation of a NOT gate. It has been shown that, in coupled semiconductor waveguide structures, it is possible to transfer the incident electron density from an input waveguide to an output waveguide using either the application of a magnetic field perpendicular to the direction of density propagation or through the addition of an applied bias across the coupled waveguide structure [1]. While the theoretical operation of the device has been shown to work, the materials in which this device is fabricated have been assumed to be perfect. Here, we investigate whether the semiconductor switching process, in different III–V semiconductor hetrostructures, remains possible in the presence of finite temperature in the material. We present the results of studies on GaAs, InSb and InAs-based semiconductor waveguide inverters, with attention given to the role of temperature.

The structure studied here is shown in Fig. 1. Two parallel waveguides, separated by an electrostatic potential barrier, are coupled via a tunnel region. The input (top) waveguide has a uniform width of 35 nm

* Corresponding author. Tel.: +1-480-965-3452.
E-mail address: matthew.gilbert@asu.edu (M.J. Gilbert).

1386-9477/03/$ - see front matter © 2003 Elsevier B.V. All rights reserved.
doi:10.1016/S1386-9477(03)00325-4

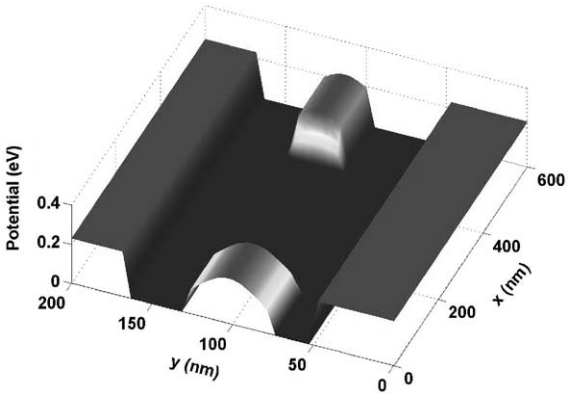

Fig. 1. Plot of the coupled waveguide structure under consideration. In this figure the coupling length between the two waveguides is 335 nm. The right-hand side of the structure ($x = 600$ nm) is defined to be the anode while the cathode is defined to be the left-hand side of the structure ($x = 0$ nm).

from start to finish, whereas the output (bottom) waveguide is narrowed at the source end, with a width of 25 nm, and then widens to a width of 45 nm after the coupling region in the middle of the structure. This wider output region assures that modes propagate through the coupling region and do not decay. The electrostatic potential barrier that separates the input and output waveguides begins with a width of 50 nm and then narrows to 25 nm after the coupling region. To achieve a more realistic potential profile for the barrier, the initial hardwall potential has been smoothed with a Gaussian distribution. The potential barrier, however, is still sufficiently high to prevent any leakage (from the input waveguide to the output waveguide) and assures all transfer of density from the input to the output occurs in the coupling region.

The Fermi energy in the structure is chosen to be 2, 9, and 19.5 meV which correspond to carrier densities of 5.6×10^{10}, 9×10^{10}, and 1.11×10^{11} cm^{-2} in GaAs, InAs, and InSb, respectively. These Fermi energies have been chosen so that only one mode is excited in the input waveguide of the structure for a given material. The input waveguide structure is wider than the output waveguide, so that the mode that is excited at this energy will not be reflected to the source end of the output waveguide. The particular dimensions of the waveguide structure can be scaled easily as long as the constraints mentioned are honored. This simulation is performed on a discretized grid using a variation of the Usuki mode matching technique via the scattering matrix [2], using a grid spacing of 5 nm.

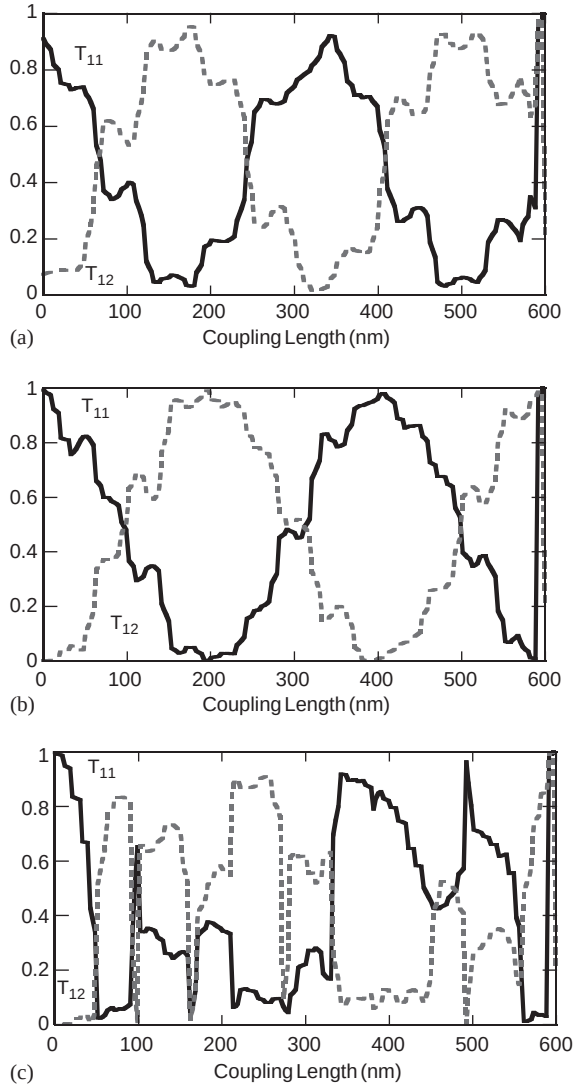

Fig. 2. (a) The individual transmissions (T_{11} and T_{12}) plotted over the coupling length between the two waveguides for GaAs. (b) The individual transmissions (T_{11} and T_{12}) plotted over the coupling length between the two waveguides for InAs. (c) The individual transmissions (T_{11} and T_{12}) plotted over the coupling length between the two waveguides for InSb.

With the Fermi energy in the system defined, we now vary the coupling length in the materials to select an initial state for the qubit. The results are shown in Fig. 2. Here the transmission to the two output

guides of the qubit is plotted against the coupling length variation for GaAs and InAs. We find that there is a very periodic pattern in the probability density transfer at each respective Fermi energy. In Fig. 2(a), for GaAs we find a period of approximately 350 nm with pure states occurring in intervals of 175 nm. In Fig. 2(b), for InAs, the period appears to be approximately 400 nm whereby we recover the superposition of the states at every 200 nm. Based on the periodicity shown in Fig. 2, we now select coupling lengths which correspond to T_{11} maxima. For GaAs, this coupling length is 335 nm and for InAs the selected coupling length is 400 nm.

In Fig. 2(c), we can see that while InSb has a regularly repeating pattern, every 150 nm, for the initial state of the qubit, it is far less stable under variations of the coupling length. While variations of the coupling length are not necessarily a concern, this suggests that InSb is unstable under energy variations as the coupling from the top guide to the bottom guide is a function of the energy relative to the coupling length. Therefore, InSb will not be discussed further.

In Fig. 3, we plot the results of adding a voltage drop, ranging from 0 to −1.0 mV for GaAs, shown in Fig. 3(a), and 0 to −7 mV for InAs, shown in Fig. 3(b), across the coupled waveguide structure with the anode at the right and the cathode at the left of the structure. This adds an extra degree of freedom to the carriers in the system, and it is no longer viable to discuss the operation of the device in terms of just the transmission and reflection of incident modes. The addition of an extra degree of freedom to the carriers excites extra output modes which are indistinguishable in the total transmission from the initially excited mode (determined by the setting of the Fermi energy). Therefore, in order to determine the extent to which our device switches from one pure state to the next, we use the Landauer formula to integrate over the individual transmissions and compute the current. We can see that in both materials, the vast majority of the current flows in the top waveguide (I_{11}) for small reverse biases. However, as we increase the reverse bias across the device, we see that the current ceases to flow in the top waveguide and transfers to the bottom waveguide (I_{12}). This occurs due to the fact that as the reverse bias is increased we begin to pinch off the top waveguide as the Fermi energy at the end of the device has been lowered to such a degree that it

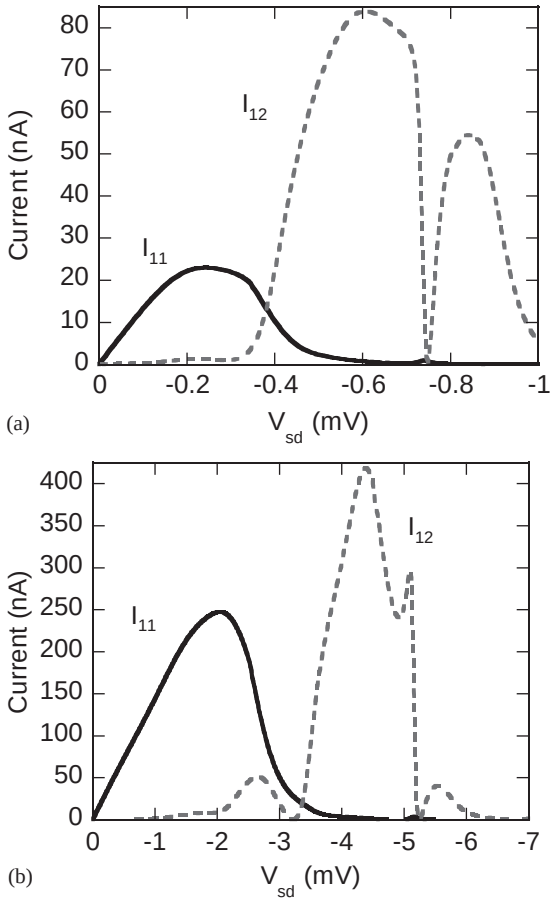

Fig. 3. (a) Output currents I_{11} and I_{12} plotted over an applied source–drain voltage ranging from 0 to −1 mV for GaAs. (b) Output currents I_{11} and I_{12} plotted over an applied source–drain voltage ranging from 0 to −7 mV for InAs.

becomes impossible for the top waveguide to sustain a propagating mode. Further, as the reverse bias increases, we are also modulating the velocity of the incoming mode. As the mode continues to slow, we see that the mode couples to the bottom waveguide as we have effectively changed the location of the coupling length that maximizes T_{12}. Moreover, as the mode continues to slow, we sweep through a highly reflective energy state which causes the null in the I–V characteristics. Finally, as the bias reaches its maximum, the Fermi energy at the output of the device reaches a level that is insufficient to sustain modes propagating in either the top or the bottom waveguide at the output of the device.

Nevertheless, to examine the effects of finite temperature on the system, we must include the difference between the Fermi level at the source and the Fermi level at the drain in the Landauer formula, as well as include the thermal effects on the energy of the incoming mode. To include thermal effects we now use

$$I(V_{sd}) = \frac{2e}{h} \int dE \cdot T(E)(f_s(E) - f_d(E)) \qquad (1)$$

to calculate the current at different applied biases where, in the above equation f_s and f_d are the values of the Fermi functions at the source contact and drain contacts respectively.

In Fig. 4, we plot the I–V characteristics of the inverter with the temperature of the system set to 1 K. We see in Figs. 4(a) and (b) that the behavior for both GaAs and InAs are quite similar to the ideal case shown in Figs. 3(a) and (b). Nonetheless, there are several differences which are important to note. First, we notice that magnitude of the current has been reduced. This can be explained by the fact that now, when the Landauer formula is applied to the transmissions to obtain the current, we have the difference between the Fermi function at the source and the Fermi function at the drain added into the convolution. This causes a lowering of the current from the ideal case. Further, we note that the position of the null in both the GaAs and InAs I–V curves has shifted position from the ideal case. This can be explained by the fact that as we impart extra energy to the system and more states contribute, it will require more reverse bias to sweep the mode through the highly reflective state that is responsible for the formation of the null. Moreover, the addition of the extra energy into the mode requires additional reverse bias to cause the device to switch from maximum transmission in the top waveguide to maximum transmission in the bottom waveguide. However, the device still switches.

Similarly, in Fig. 5 we raise the temperature once again to 2 K and plot the resultant I–V characteristics. Once again, we see that both the applied bias where the device switches from transmission to the top waveguide to transmission to the bottom waveguide has been increased. Further, we also see that the position of the nulls has also shifted to higher applied reverse biases. Nonetheless, when enough bias is applied to the structure, the electron probability density switches from the top waveguide to the bottom waveguide.

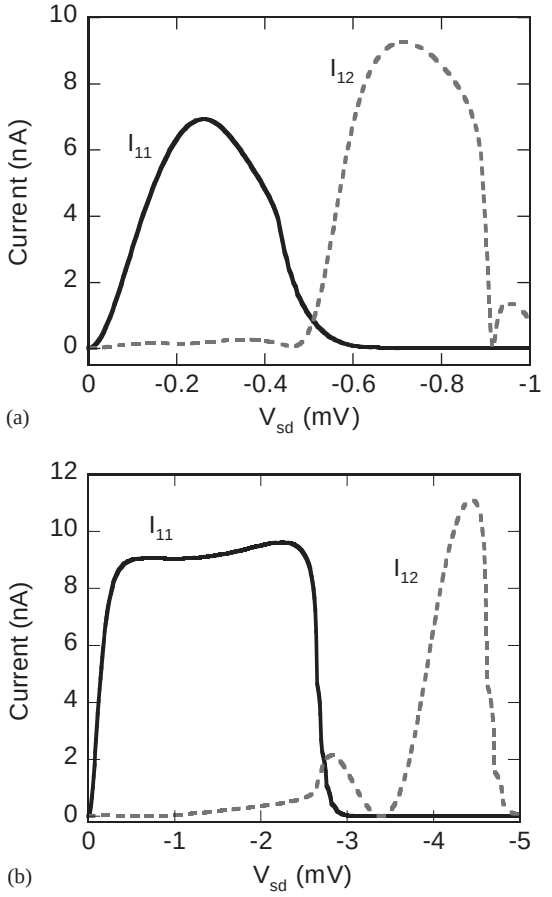

Fig. 4. (a) Output currents I_{11} and I_{12} plotted over an applied source–drain voltage ranging from 0 to −1.5 mV for GaAs at a temperature of 1 K. (b) Output currents I_{11} and I_{12} plotted over an applied source–drain voltage ranging from 0 to −5.5 mV for InAs at a temperature of 1 K.

In Fig. 6, we raise the temperature to 4.2 K. At 4.2 K the excess energy imparted to the system becomes enough to excite a second mode in both the GaAs, Fig. 6(a), and in InAs, Fig. 6(b). The excitation of a second mode in the system changes the operation of the device in that we no longer have a null in the system that was prevalent at lower temperatures. This second mode does not couple from the top waveguide to the bottom waveguide at the same applied bias as the first mode. Therefore, when the voltage is swept, we no longer see the characteristic null in the I–V curve. In addition to this, we also see that we require a larger applied bias to switch the electron probability

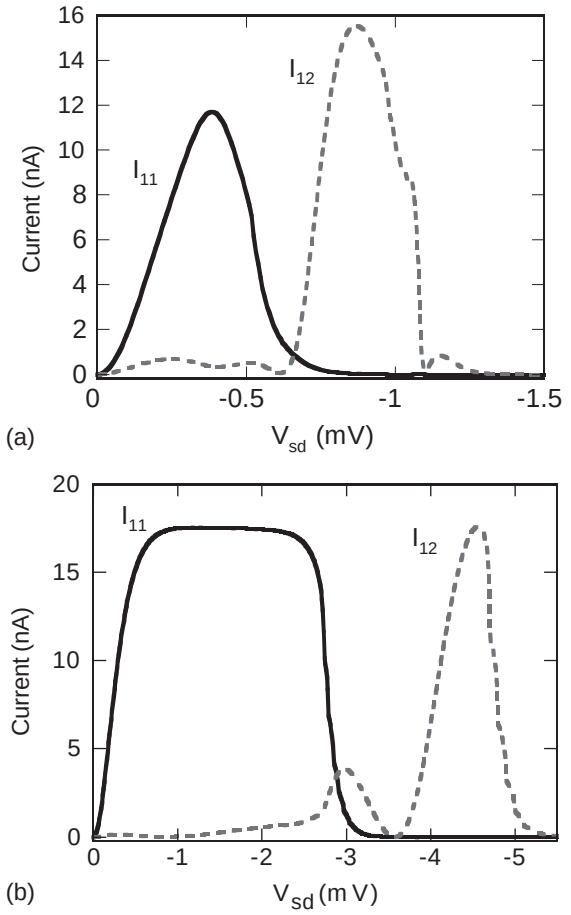

Fig. 5. (a) Output currents I_{11} and I_{12} plotted over an applied source–drain voltage ranging from 0 to −1.5 mV for GaAs at a temperature of 2 K. (b) Output currents I_{11} and I_{12} plotted over an applied source–drain voltage ranging from 0 to −6 mV for InAs at a temperature of 2 K.

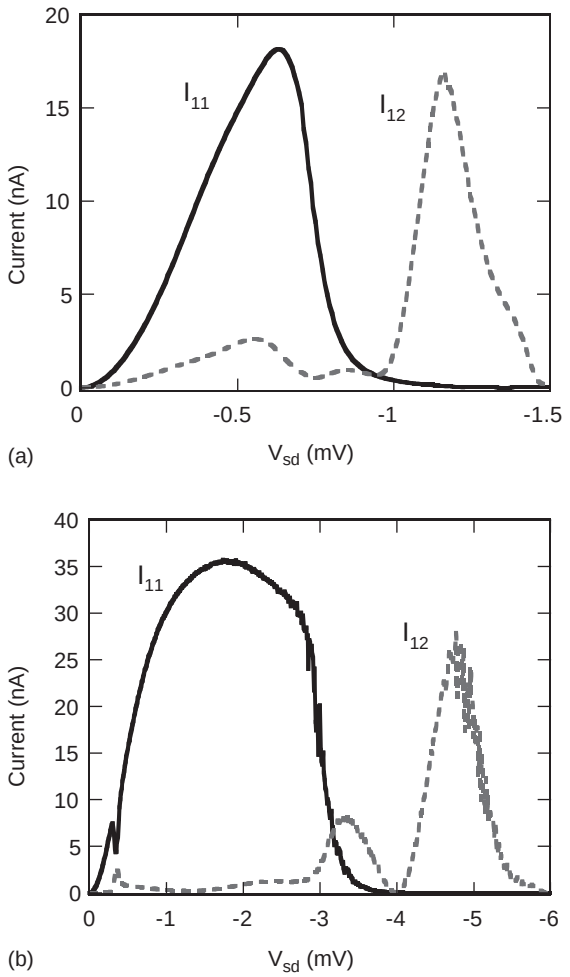

Fig. 6. (a) Output currents I_{11} and I_{12} plotted over an applied source–drain voltage ranging from 0 to −1.5 mV for GaAs at a temperature of 4.2 K. (b) Output currents I_{11} and I_{12} plotted over an applied source–drain voltage ranging from 0 to −6 mV for InAs at a temperature of 4.2 K.

density from the top waveguide to the bottom waveguide. This is quite understandable given the fact that we now have a second higher energy mode propagating in the system. Therefore, even though the first excited mode may couple at lower applied biases, the second mode may still be transmitting mainly to the output of the top waveguide. Nonetheless, as the reverse bias is increased, we see that the current does switch from the top waveguide to the bottom waveguide thereby completing the inversion process.

In Fig. 7, we raise the temperature to 10 K and plot the resultant I–V characteristics. At 10 K, the device operates much the same way as in the case of Fig. 6 where the temperature of the device has been set to 4.2 K. We have excited two modes in the system and, as we can see, there are no nulls because of the presence of the second mode in the system. Furthermore, as expected, the situation at 10 K requires the addition of extra reverse bias to cause both of the modes to couple. Nevertheless, the operation of the device is still intact.

In conclusion, we find that the addition of finite temperature to the semiconductor waveguide inverter

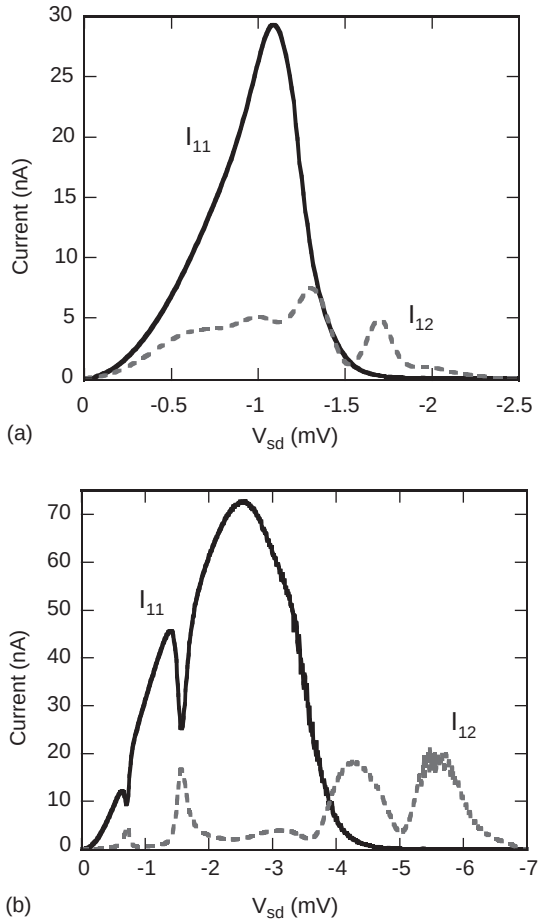

Fig. 7. (a) Output currents I_{11} and I_{12} plotted over an applied source–drain voltage ranging from 0 to −2.5 mV for GaAs at a temperature of 10 K. (b) Output currents I_{11} and I_{12} plotted over an applied source–drain voltage ranging from 0 to −7 mV for InAs at a temperature of 10 K.

does not cause the device to stop functioning. But that is not to say that temperature has no effect on the operation of the device at all. In truth, care must be taken when setting the operational voltages of the device. The addition of temperature causes the position of the highly reflective null states to shift up in energy. An unwise choice of operating voltage results in poor device operation as the null may shift towards the operating voltage. Further, with higher temperature comes the need for higher applied biases to cause the device to invert. Therefore, if the chosen operating voltage is too low for a given operating temperature, then the device will not operate as designed. However, if caution is taken when setting the operational voltage of the semiconductor waveguide inverter, then finite temperature does not effect the overall operation of the device.

This work is supported by the Office of Naval Research.

References

[1] M.J. Gilbert, R. Akis, D.K. Ferry, App. Phys. Lett. 81 (2002) 4284.
[2] T. Usuki, M. Saito, M. Takatsu, R.A. Kiehl, N. Yokoyama, Phys. Rev. B 52 (1995) 8244.